Field Dependence of Solvent Proton and Deuteron NMR Relaxation Rates of the Manganese(II) Binding Site of Chloroplast Coupling Factor 1[†]

Alice E. Haddy and Robert R. Sharp*
Department of Chemistry, The University of Michigan, Ann Arbor, Michigan 48109

Received July 19, 1988; Revised Manuscript Received November 18, 1988

ABSTRACT: The high-affinity Mn(II) binding site of chloroplast coupling factor 1 (CF_1), the ATP synthase of higher plants, was studied by field-dependent water proton and deuteron NMR spin-lattice relaxation analysis. Magnetic field dependence of the solvent ^1H relaxation rate (R_1) contains information about the number (q) and the residence lifetime (τ_m) of water molecules within the inner coordination sphere of bound Mn(II) and the spectral density function of the magnetic dipole interaction of the water protons and the Mn(II) ion. Chemical analysis of endogenous nucleotides and metals in the purified enzyme revealed about 1.1-1.3 mol of ADP, 0.1-0.2 mol of ATP, and 1.3 mol of Mg(II) per mole of CF_1; no Mn(II) was detected. The enzyme bound 0.7 molar equiv of Mn(II) in nonlabile sites and at least 1 additional molar equiv of Mn(II) in a labile site. ^1H NMR relaxation studies were conducted on solutions of purified CF_1 and $MnCl_2$ at binding ratios of 0.47, 0.89, and 1.3 and ^1H Larmor frequencies between 4 and 62 MHz. The R_1 data were extrapolated to zero Mn(II) to CF_1 binding ratio in order to characterize the first binding site occupied by Mn(II). This site contains a single water molecule in chemical exchange equilibrium with the solvent, for which the mean residence time is 330 ns. The electron spin relaxation time of bound Mn(II) is long, indicating high site symmetry. The Mn(II) site appears to have approximate tetrahedral symmetry with three protein ligands and one exchangeable water ligand. This Mn(II) binding site is filled when the divalent metal concentration exceeds the substrate concentration, and it appears to have an inhibitory effect on ATPase activity.

Spinach chloroplast coupling factor 1 (CF_1),[1] the photosynthetic adenosinetriphosphatase, requires a divalent metal cofactor for both synthesis and hydrolysis of ATP. Kinetic analyses of the ATPase reaction indicate that the substrate for hydrolysis is a metal-nucleotide complex (Hochman & Carmeli, 1981a,b; Hiller & Carmeli, 1985). While the metal cofactor of CF_1 is generally believed to be Mg(II) in vivo, Mn(II), at concentrations less than about 1 mM, has been found to be a highly effective cofactor for ATPase activity (Hochman & Carmeli, 1981a).

Mn(II) is an $S = {}^5/_2$ paramagnetic ion with relaxation properties that make it a valuable NMR (Haddy et al., 1985) and ESR (Hiller & Carmeli, 1985) probe of metal binding to CF_1. These studies have demonstrated the presence on isolated CF_1 of two to three high-affinity ($K_d < 20\ \mu M$) Mn(II) binding sites, which exhibit positive cooperativity. In addition, several sites with relatively low binding affinity ($K_d > 40\ \mu M$) have been reported. While progress has been made in understanding the equilibrium binding properties of divalent cations and nucleotides to CF_1, very little information is available concerning the inner sphere environment of the bound metal. A recent study of the manganese EXAFS has provided useful information in this regard (Carmeli et al., 1986).

Another experimental probe of the manganese binding site is provided by the NMR relaxation properties of solvent protons and deuterons. When the bulk solvent is in rapid chemical exchange equilibrium with sites in the first coordination sphere of enzyme-bound Mn(II), the metal ion acts as a relaxation trap which, at micromolar concentrations, can determine the magnetic relaxation properties of nuclei in the bulk solvent pool. Thus, the solvent $^1H/^2H$ NMR signals provide a sensitive probe of magnetic interactions in the first coordination sphere of enzyme-bound manganese. Mechanistic analyses of these interactions are in general facilitated by measurements over a range of magnetic field strengths. Used in combination with data from the two hydrogen isotopes, the magnetic field dispersion profile of the solvent proton spin-lattice relaxation rate, R_1, provides information concerning (1) the number of exchangeable solvent molecules bound to the metal, (2) the chemical exchange kinetics between these sites and the bulk solvent, and (3) the spectral density function of the magnetic dipole interaction between bound water protons and the Mn(II) ion.

Detailed field-dependent R_1 studies have been reported previously for several mangano-enzymes, including Mn(II)-carboxypeptidase A (Navon, 1970; Koenig et al., 1971), Mn(II)-pyruvate kinase (Navon, 1970), Mn(II)-carbonic anhydrase (Lanir et al., 1975), and Mn(II)-concanavalin A (Koenig et al., 1973; Brown et al., 1977). In this and the following paper (Haddy et al., 1989), we report an analysis of the magnetic field dependence of the solvent proton relaxation rate in solutions of binary Mn(II)-CF_1 and of ternary Mn(II)-nucleotide-CF_1 complexes.

Nucleotide binding sites on isolated CF_1 have been characterized by work in a number of laboratories. Hammes and co-workers [see, for example, Leckband and Hammes (1987)] have classified three high-affinity ($K_d < 20\ \mu M$) nucleotide binding sites, termed sites 1, 2, and 3. Site 1 is an ADP binding site with the highest affinity for ADP (Carlier & Hammes, 1979; Bruist & Hammes, 1981). This site is usually occupied in isolated CF_1 and is not depleted by extensive dialysis or gel filtration chromatography, although ADP in this site does exchange with medium nucleotides. Site 2 binds

---

[†] This work was supported by the U.S. Department of Agriculture in the form of a research grant (83 CRCR 1 1339).

* Author to whom correspondence should be addressed.

[1] Abbreviations: CF_1, chloroplast coupling factor 1; AdN, adenine nucleotide.

0006-2960/89/0428-3656$01.50/0

Mg(II)–ATP with high affinity and appears to be without catalytic function in the activated ATPase (Bruist & Hammes, 1981; Leckband & Hammes, 1987). Mg(II)–ATP bound to site 2 resists depletion by gel filtration chromatography. This site is usually unoccupied in the latent enzyme following isolation, indicating that precipitation of the enzyme with $(NH_4)_2SO_4$ removes metal–ATP (Bruist & Hammes, 1981). Mn(II)–ATP, like Mg(II)–ATP, probably binds to this site since Hochman and Carmeli (1981a) found an increase in high-affinity Mn(II) binding sites in the presence of ATP. Site 3 is a lower affinity ($K_d \approx 1$–$4\ \mu$M), probably catalytic (Bruist & Hammes, 1981; Leckband & Hammes, 1987), binding site with affinity for both ADP (in both the presence and absence of divalent metal) and ATP [in the presence of Mg(II)]. Two ADP binding sites with measurable dissociation constants ($K_d \approx 1$–$4\ \mu$M) have been reported by numerous laboratories (Girault et al., 1973; Cantley & Hammes, 1975; Banai et al., 1978; Carlier & Hammes, 1979; Bruist & Hammes, 1981). These probably correspond to sites 2 and 3 since only one of these ADP sites is detected when site 2 is occupied by Mg(II)–ATP (Bruist & Hammes, 1981).

Isolated CF$_1$ contains binding sites not only for nucleotides and metal–nucleotide complexes, as described above, but also for divalent metal ions that are unaccompanied by nucleotide. Chemical analyses have indicated that in the absence of added nucleotides the divalent metals Mg(II) and Mn(II) can bind with very high affinity in significant molar excess over endogenous nucleotide (Hiller & Carmeli, 1985; Girault et al., 1982). This result is confirmed in experiments reported below. The functional role of tight metal ion binding sites is not clear at present. It may be significant that while Mg(II) and Mn(II) are cofactors for ATP hydrolysis, both of these metal ion inhibit hydrolysis when the metal concentration exceeds that of the nucleotide substrate (Hochman et al., 1976; Hochman & Carmeli, 1981a). Mg(II) bound to CF$_1$ appears to be involved in the formation of a state of the enzyme that is inhibited with respect to ATPase activity; removal of Mg(II) from heat-activated CF$_1$ by incubation with EDTA correlates with the relief of inhibition of ATPase activity as well as with the removal of ADP from nucleotide site 1 (Feldman & Boyer, 1985). Thus, it is possible that bound divalent metal cations that are uncoordinated by nucleotide have an inhibitory, as opposed to a catalytic, function.

The experiments reported here investigate the properties of high-affinity Mn(II) binding sites that are present on latent CF$_1$ which has been depleted of labile nucleotides by extensive gel filtration chromatography. Because of the cooperative interaction between metal ion binding sites and the heterogeneity of nucleotide binding sites, attention has been focused on the Mn(II) which binds at the lowest Mn(II)/CF$_1$ mole ratios. Mn(II) in this site is nonlabile during prolonged gel filtration. To isolate NMR relaxation contributions due to this high-affinity site, we have measured the Mn(II) concentration dependence of the proton relaxation profiles, using substoichiometric [0.5 mol of Mn(II)/mol of CF$_1$] to superstoichiometric [1.5 mol of Mn(II)/mol of CF$_1$] concentrations of added Mn(II), and extrapolated the results of the analysis to zero Mn(II) bound per CF$_1$. This extrapolation provides information on the metal binding site that is occupied in the low Mn(II)/CF$_1$ limit. Analysis of the data for Mn(II)/CF$_1$ > 1 addresses the question of heterogeneity in the population of bound Mn(II).

MATERIALS AND METHODS

Spinach chloroplast coupling factor 1 (CF$_1$) was prepared essentially as described previously (Frasch & Selman, 1982) with the following modifications. Thylakoids were washed 5 times in 10 mM sodium pyrophosphate buffer to remove ribulosebisphosphate carboxylase before extraction of CF$_1$ with sucrose–Tris–Tricine buffer. Extracted CF$_1$ which had been adsorbed onto DEAE-Sephadex A-50 was purified in a single step by elution with a linear gradient of 100–300 mM $(NH_4)_2SO_4$. The protein was stored as a precipitate in 55% saturated $(NH_4)_2SO_4$ at 4 °C.

Table I: Binding of Mn(II) and Nucleotides That Could Not Be Removed by Gel Filtration[a]

		bound (mol/mol of CF$_1$)			
[CF$_1$] (μM)	[MnCl$_2$] (μM)	ADP	ATP	Mg	Mn(II)
34	0	nd	nd	1.3	0
43	0	1.1	0.22	nd	nd
27	52	1.1	0.22	nd	0.69
39[b]	0	1.3	0.09	nd	nd
14[b]	49	nd	nd	nd	0.70

[a] CF$_1$, pretreated by gel filtration, was incubated with MnCl$_2$ where indicated and then freed of dissociable metal and analyzed as described under Materials and Methods. Errors for nucleotide determinations were 10% or less. Errors for Mn(II) determinations were about 5%. The error for the Mg determination was about 10%. [b] These samples were treated with Chelex 100 before incubation with MnCl$_2$ (where relevant) as described under Materials and Methods. nd = not determined.

The protein used for all experiments gave Ca(II)–ATPase V_{max} values of 30–35 μmol (mg of CF$_1$)$^{-1}$ min^{-1} after activation at 60 °C for 4 min in the presence of 5 mM DTT. Protein was quantitated by using the method of Lowry et al. (1951) using a BSA standard; the molecular weight of CF$_1$ was assumed to be 400 000 (Moroney et al., 1983). Latent CF$_1$ was prepared by dissolving the ammonium sulfate precipitated protein in 40 mM Tris-HCl buffer, pH 8.0, and then passing it over a 1 × 28 cm Sephadex G-50 column which had been equilibrated in the same buffer. This treatment removed all but 1.1–1.3 mol of ADP and 0.1–0.2 mol of ATP per mole of CF$_1$ (see Results). The enzyme was concentrated by pressure dialysis using a 100 000 molecular weight cutoff Millipore filter. Except for the first three samples of Table I, the enzyme was then passed rapidly over a 3-mL Chelex 100 column, prepared in a 3 cm^3 syringe, equilibrated in Tris buffer, and concentrated again. The ATPase activity of enzyme treated in this way remained at control levels.

Quantitation of Bound Mn(II), Nucleotides, and Mg Which Dissociated Slowly (Table I). Enzyme was passed over a gel filtration column (1 × 28 cm Sephadex G-50) and, where indicated, treated with Chelex 100 as described above to remove dissociable and unbound storage substances. After a concentration step, the enzyme (14–43 μM) was either analyzed as described below or incubated with the indicated concentration of MnCl$_2$ for 50–60 min at room temperature (22–23 °C). Labile Mn(II) was then removed by a second passage over the reequilibrated Sephadex G-50 column, which took about 20 min, and the enzyme was reconcentrated.

In order to quantitate bound nucleotides, Mn(II), and Mg, 4–16 μM enzyme was denatured in 0.67 M HCl at room temperature. The supernatant liquid containing nucleotides, Mn(II), and Mg was separated from the precipitate by centrifugation. For nucleotide analyses, aliquots of the acid supernatant were diluted about 15-fold using the appropriate buffer and brought to the proper pH with KOH. ADP was measured by using the pyruvate kinase/lactate dehydrogenase coupled enzyme assay; ATP was measured by using the hexokinase/glucose-6-phosphate dehydrogenase coupled enzyme assay (Williamson & Corkey, 1969). Fluorescence changes were compared to internal ADP and ATP standards.

Free Mn(II) in CF_1 samples was measured from the amplitude of the six-line ESR signal of hexaaquo-Mn(II); measurements were made at X-band on a Bruker Model ER200 spectrometer, with microwave power of 101 mW and modulation amplitude of 25 G ($p-p$). Total Mn was measured by ESR on the acid extract of the same samples. Magnesium in the acid supernatant was determined by graphite furnace atomic absorption spectroscopy (Perkin-Elmer Model 2380).

Spin–Lattice Relaxation Measurements. Spin–lattice relaxation rates, $R_1 = 1/T_1$, of solvent water protons or deuterons were measured by using a modified triplet sequence $[180_0–\tau_1–(90_0–\tau_2–180_\pi–\tau_2–90_0–\tau_1)_n]$ as described previously (Sharp, 1972; Haddy et al., 1985). Proton relaxation rates were measured at Larmor frequencies between 4 and 62 MHz (25 °C) in order to generate magnetic field dependence profiles. ^2H and ^1H relaxation rates were measured at 12.63 MHz on samples containing about 3/1 $^2H_2O/^1H_2O$ in order to provide unique analyses of the dispersion profile data.

The total measurement time for a single set of dispersion profile samples was 12 h. Measurements at 20.63 MHz and below were made on one day using 100-μL samples; measurements at 20.63 MHz and above were made on a second day using 80-μL samples of freshly prepared enzyme. The 20.63-MHz point measured on the second day was normalized to the equivalent point of the first day, thereby providing a correction for small variations due to slight concentration differences. A check on the stability of samples indicated a slight decrease of up to 8% in R_1 over the 12-h measurement period.

Analysis of NMR Relaxation Data. Nuclear magnetic spin–lattice relaxation in the presence of paramagnetic Mn(II) was analyzed according to the Solomon–Bloembergen–Morgan (SBM) equations. The observed paramagnetic relaxation rate, $1/T_{1p}$, depends on the number, q, the residence time, τ_m, and the relaxation rate, $1/T_{1m}$, of water molecules within the inner coordination sphere of Mn(II):

$$\frac{1}{T_{1p}} = \sum_i \frac{q_i E_i}{55.5[(T_{1m})_i + (\tau_m)_i]} \tag{1}$$

where the sum is over classes of manganese environments, including those of free Mn^{2+} and the binding sites on CF_1. The present analysis focuses primarily on the metal site that is occupied in the limit of low added Mn(II). In this limit, only a single term is appreciable in eq 1.

For NMR–PRE studies involving aqueous Mn(II), ^1H relaxation is dominated by magnetic dipole interactions (Koenig et al., 1971), and the equation for spin–lattice relaxation has the form (assuming $\omega_s \gg \omega_I$)

$$\frac{1}{T_{1m}} = \frac{B}{r^6}\left[\frac{7\tau_{c2}}{1 + (\omega_s\tau_{c2})^2} + \frac{3\tau_{c1}}{1 + (\omega_I\tau_{c1})^2}\right] \tag{2}$$

where $B = (2/15)(h\gamma_I\gamma_s)^2 S(S+1)$. I and S are the ^1H and electron spins, $\omega_{I,s}$ and $\gamma_{I,s}$ are the Larmor frequencies and magnetogyric ratios, respectively, r is the separation of the spins, and $\tau_{c1,2}$ are the correlation times for the dipolar interaction in the longitudinal and transverse planes, respectively. The time dependence of the dipolar interaction is given as a sum of rates of modulating processes:

$$\frac{1}{\tau_{c1}} = \frac{1}{\tau_{s1}} + \frac{1}{\tau_m} + \frac{1}{\tau_r} \tag{3}$$

τ_{s1} is the electron spin relaxation time, τ_m is the mean residence time of protons in the bound site, and τ_r is the reorientational correlation time.

The magnetic field dependence of the NMR–PRE arises in part from the explicit dependence of the eq 2 on the transition frequencies, ω_I and ω_s, of the I and S spins. In addition, an implicit magnetic field dependence arises when $\omega_s\tau_{s1} > 1$. The electron spin relaxation rate, $1/\tau_{s1}$, contains an implicit magnetic field dependence and is usually written in the form (Bloembergen & Morgan, 1961)

$$\frac{1}{\tau_{s1}} = \frac{0.2}{\tau_s^{\circ}}\left[\frac{1}{1 + (\omega_s\tau_v)^2} + \frac{4}{1 + (2\omega_s\tau_v)^2}\right] \tag{4}$$

where τ_s° is the low-field limiting value of τ_{s1}.

Physically, the quantity in brackets is the spectral density function of vibrational motions which modulate the ZFS tensor through distortions of the first coordination sphere. For aqueous cations, measured values of τ_v lie on a vibrational time scale, ca. 3×10^{-12} s (Friedman et al., 1975; Koenig et al., 1974). A correlation time of this magnitude results in a field-independent electron spin relaxation time, i.e., $\tau_{s1} = \tau_s^{\circ}$.

Experimentally, τ_{s1} in CF_1 solutions has been found to consist of both field-dependent and field-independent components (see Results). The field-dependent component results from a motion, the correlation time of which is difficult to measure accurately, but which is substantially longer than 10 ps, in the range of 50–200 ps or more. Long correlation times for electron spin relaxation have also been reported for carboxypeptidase A (Navon, 1970; Koenig et al., 1971), pyruvate kinase (Navon, 1970), and concanavalin A (Koenig et al., 1973; Brown et al., 1977). We interpret these long correlation times as reflective of relatively slow "breathing" motions of the protein, low-frequency acoustical vibrational modes involving cooperative motions of many atoms in the neighborhood of the bound metal ion. These low-frequency motions correspond to collective motions of atoms within proteins which have been revealed by computer simulation studies; such studies have found that collective motions occur on time scales ranging from 1 to 10 ps or longer (for small proteins) as opposed to local motions of atoms which occur on a subpicosecond time scale (Karplus et al., 1983). If the low-frequency modes produce large-amplitude distortions in the Mn(II) coordination sphere that are not effectively randomized by high-frequency modes, then the two types of motions will contribute independently to $1/\tau_{s1}$. Accordingly, we have expressed the electron spin relaxation time as a sum of two terms, one field-dependent and one field-independent, describing respectively the low-frequency ("acoustical") and high-frequency ("optical") distortional motions for which the correlation times are τ_d and τ_v, respectively. In the range of magnetic field strengths used here, where $\omega_s < 2.5 \times 10^{11}\ s^{-1}$, the field dependence in the electron spin relaxation rate arises predominantly from the acoustical term and is given by

$$\frac{1}{\tau_{s1}} = \frac{0.2}{\tau_{s,d}^{\circ}}\left[\frac{1}{1 + (\omega_s\tau_d)^2} + \frac{4}{1 + (2\omega_s\tau_d)^2}\right] + \frac{1}{\tau_{s,v}} \tag{5}$$

Corrections to the Observed Relaxation Rate for Diamagnetic Contributions and Contributions from Hexaaquo-Mn(II). In order to calculate the paramagnetic relaxation rates, $1/T_{1p}$, due to Mn(II) binding to CF_1, the measured relaxation rates of Mn(II)–CF_1 solutions were corrected for effects of the Mn(II)-free protein and for unbound Mn^{2+}. The concentration of the latter was determined directly in protein-containing solutions by ESR. The molar relaxivity of $Mn(H_2O)_6^{2+}$ was calculated following Bloembergen and Morgan (1961).

Companion Analysis of Proton and Deuteron Relaxation Data. Companion measurements of ^{1}H and ^{2}H R_1's provide a direct determination of the physical parameters of interest. Using the fact that $T_{1m}{}^p/T_{1m}{}^d = (\gamma^d/\gamma^p)^2$, where γ is the nuclear magnetogyric ratio and the superscripts denote the hydrogen isotopes, we can solve eq 1 for τ_m and q as follows:

$$\tau_m = T_{1m}{}^p\left[\frac{(\gamma^p/\gamma^d)^2 T_{1p}{}^p - T_{1p}{}^d}{T_{1p}{}^d - T_{1p}{}^p}\right] \tag{6}$$

$$q = T_{1m}{}^p\left\{\frac{55.5[(\gamma^p/\gamma^d)^2 - 1]}{E(T_{1p}{}^d - T_{1p}{}^p)}\right\} \tag{7}$$

Use of these equations requires an experimental determination of $T_{1m}{}^p$, which is best obtained from the field dispersion profile of the ^{1}H data. For Mn(II)–enzymes, this profile generally exhibits two marked dispersions, corresponding to the two terms of eq 2 (Koenig et al., 1971, 1973; Brown et al., 1977). The dispersion at higher field, i.e., that which occurs when $\omega_I\tau_{c1} \approx 1$, has a more complicated field dependence than that at $\omega_S\tau_{c2} \approx 1$ due to an implicit magnetic field dependence in the electron spin relaxation time τ_{s1} at high field as given by eq 5. The qualitative form of the higher field dispersion in solutions of Mn(II)–enzymes is frequently observed to be a local maximum in R_1 that is centered near the frequency $\omega_{I,m} = 1/\tau_{c1}$. The proton Larmor frequency at the R_1 maximum provides a direct determination of the spectral density function with an accuracy of about 30%. At this point

$$\frac{1}{T_{1m}{}^p} = \frac{B}{r^6}\left[\frac{3\tau_{c1}}{1 + (\omega_I\tau_{c1})^2}\right] = \frac{B}{r^6}\left(\frac{3}{2\omega_{I,m}}\right) \tag{8}$$

Companion ^{1}H and ^{2}H relaxation measurements are conveniently made at the field strength of the local $1/T_{1p}$ maximum. At this field, eq 6–8 can be solved for q and τ_m in terms of measured relaxation times:

$$\tau_m = \frac{r^6}{B}\left(\frac{2\omega_{I,m}}{3}\right)\left[\frac{(\gamma^p/\gamma^d)^2 T_{1p}{}^p - T_{1p}{}^d}{T_{1p}{}^d - T_{1p}{}^p}\right] \tag{9}$$

$$q = \frac{r^6}{B}\left(\frac{2\omega_{I,m}}{3}\right)\left\{\frac{55.5[(\gamma^p/\gamma^d)^2 - 1]}{E(T_{1p}{}^d - T_{1p}{}^p)}\right\} \tag{10}$$

Starting with approximate values of T_{1m}, τ_m, and q from eq 8–10, the full parameter set, which includes the correlation times $\tau_{s,v}$ and $\tau_{s,d}{}^o$, was refined by least-squares fits of the field-dependent proton R_1 data to eq 1, 3, 4, and 6. The value for r, the separation between nuclear and electron spins, was taken to be the crystallographic value for hexaaquo-Mn(II), 2.77 Å (Dwek, 1973).

This method of combining ^{1}H and ^{2}H data is advantageous in that the central parameters of interest, namely, q, τ_m, and T_{1m}, are determined without reliance upon the detailed form of the spectral density function. The single piece of information that is required from the shape of the dispersion profile is the ^{1}H Larmor frequency at the R_1 maximum, which provides an unambiguous determination of τ_{c1} and of the magnitude of the spectral density function at that point. In contrast, the correlation times, τ_d and $\tau_{s,v}$, which determine the electron spin relaxation properties, are closely linked to the field dependence of the proton R_1 data and are determined by a fit of the data to the full set of equations. The use of eq 8–10 to provide starting values for q, τ_m, and T_{1m} tends to separate the determination of this parameter set from that comprising the correlation times in eq 5. In this way, the possibility of ambiguities arising from multiple-error minima in the general multiparameter fit is largely eliminated.

Starting values were also evaluated for the correlation times of eq 3 and 5. τ_r has been measured directly (Schinkel & Hammes, 1986), but this parameter appears only as a small correction (<3%) in the sum ($1/\tau_m + 1/\tau_{s1} + 1/\tau_r$) and is of little significance. τ_d was estimated roughly from the fact that τ_{s1} is already in the field-dependent region on the low-field side of the local maximum in R_1, which implies that $\tau_d \geq 50$ ps. Fits were conducted by setting τ_d to various values between 50 and 200 ps and allowing variation in $\tau_{s,d}{}^o$ and $\tau_{s,v}$. In the field-dependent region of τ_{s1}, τ_d and $\tau_{s,d}{}^o$ enter the theory approximately as the product ($\tau_d{}^2\tau_{s,d}{}^o$) and were accordingly found to be strongly covariant. The other parameters showed little covariance with τ_d, and their iterated values were largely independent of the initial choice for this parameter.

RESULTS

Quantitation of Metals and Nucleotides Bound to CF$_1$. Table I gives the levels of adenine nucleotides present on latent CF$_1$ following purification by extensive gel filtration chromatography and exposure to Chelex 100, which is a very high affinity divalent cation-exchange resin. Two enzyme preparations were examined and gave similar results. Table I shows results for the second preparation which was also used for the NMR experiments presented below. Enzyme treated by extensive gel filtration retained 1.1 mol of ADP and 0.2 mol of ATP per mole of CF$_1$ (Table I, row 2). Passage of the enzyme over a short column of Chelex 100 did not alter the total endogenous nucleotide, although the ATP/ADP ratio appeared to decrease significantly (Table I, row 4).

Endogenous Mg^{2+} was present in our CF$_1$ preparations at a level of about 1.3 mol/mol of CF$_1$ (Table I, row 1). This metal was not removed by inclusion of EDTA in the storage buffer, by gel filtration procedures using Sephadex G-50, or by treatment of the enzyme with Chelex 100. This endogenous Mg(II) level is similar to that reported by Hiller and Carmeli (1985) but significantly higher than that found by Girault and co-workers (Girault et al., 1982), who reported no more than 0.6 mol/mol of CF$_1$ following a somewhat more severe preparative procedure in which the buffers used for EDTA extraction and purification did not contain added adenine nucleotides.

Thylakoid membranes have been reported to contain a very high-affinity manganese binding site which appears not to be located in the oxygen evolving system and is not released by NH$_2$OH/EDTA extraction (Yocum et al., 1981). Because of the established divalent metal ion requirement of ATP synthesis, and the high levels of endogenous Mn(II) that are present in chloroplasts in vivo, it was proposed that this Mn(II) is bound to CF$_1$. We therefore examined, using ESR spectroscopy, the endogenous Mn(II) content of isolated CF$_1$ after gel filtration treatment. No endogenous manganese was found within our detection limits of about 0.05 Mn(II)/CF$_1$ (Table I, row 1).

Amounts of bound Mn(II) and nucleotide were also determined after incubation of CF$_1$ with MnCl$_2$, followed by a second passage over a Sephadex G-50 column (1 × 28 cm) to remove labile low molecular weight species. This second gel filtration step did not alter the amounts of bound ADP and ATP (Table I, row 3). In addition, nonlabile Mn(II) was found at a level of 0.69 mol/mol of CF$_1$. (The practical definition of ligand lability in these experiments is the duration

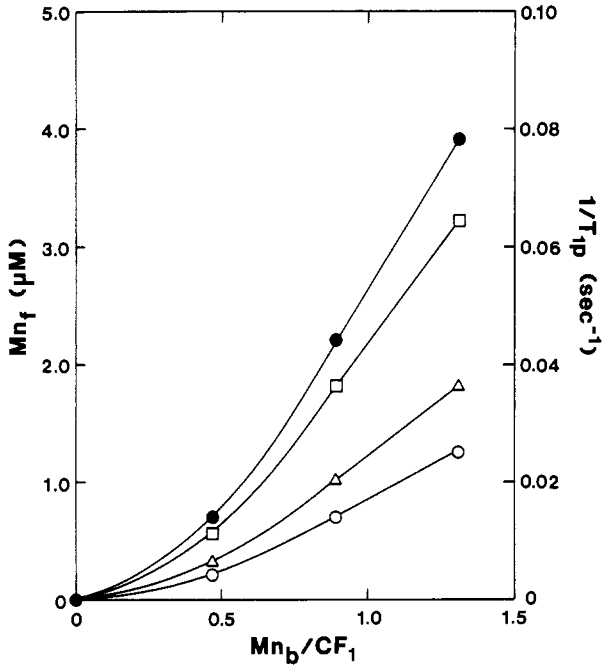

FIGURE 1: Dependence of the free Mn^{2+} concentration ($[Mn]_f$) and the corresponding paramagnetic relaxation rates due to free Mn(II) ($1/T_{1p}$) on the binding ratio of Mn(II) to CF_1 (Mn_b/CF_1). The free Mn^{2+} concentrations (closed circles, left-hand scale) correspond to those of the four solutions used for the field dependence study. The relaxation rates due to free Mn^{2+} (right-hand scale) are shown at three representative proton frequencies: 4.9 MHz (open squares); 15.2 MHz (open triangles); and 61.6 MHz (open circles).

of the gel filtration procedure, approximately 20 min.) We also investigated the possibility that prior treatment of the enzyme with the exchange resin Chelex 100 might increase the amount of bound Mn(II) by removing endogenous Mg(II). Treatment with Chelex did not significantly alter the results, however (Table I, row 5).

The total Mn(II) bound to CF_1 during the NMR experiments, including both labile and nonlabile, was measured by using the six-line hyperfine ESR signal of Mn^{2+} (Figure 1, closed circles). The six-line signal measures free $Mn(H_2O)_6{}^{2+}$ and, by difference with added $MnCl_2$, the total bound Mn(II). The data of Figure 1 suggest the existence of two populations of bound Mn(II). The higher affinity site appears to saturate when the bound Mn(II) per CF_1 is about 0.5 or more, which agrees fairly well with the quantitation of bound Mn(II) that resists removal by gel filtration (Table I). At higher mole ratios of bound Mn(II) to CF_1, Mn(II) was bound to a lower affinity population of sites which had a binding constant in the low micromolar range. These data are similar to those of Hochman and Carmeli (1981a), who also found one high-affinity site and several low-affinity sites for Mn(II) although all of the sites observed in that study had lower affinities than those reported here.

In summary, these data indicate the presence of several divalent metal sites. An average of two divalent metal ion binding sites on latent CF_1 were nonlabile over a time scale of tens of minutes. These were occupied by 1.3 molar equiv of Mg(II), which was present as endogenous metal in the isolated enzyme, and by 0.7 mol of added Mn(II). A significant portion of this metal was present in some form other than as metal–nucleotide complexes, since the total concentration of nonlabile metal ion exceeded the concentration of bound nucleotide. In addition to these two nonlabile binding sites, at least one other high-affinity Mn(II) binding site, with a dissociation constant in the low micromolar range, was present. At the highest mole ratios of added Mn(II) to CF_1 studied (1.5 mol/mol), 1.3 mol of metal/mol of CF_1 was bound without an equivalent amount of nucleotide.

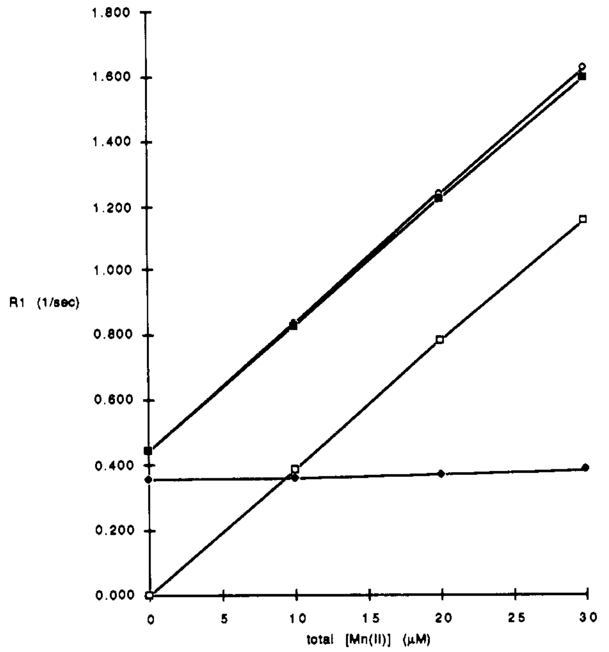

FIGURE 2: Corrections to the observed relaxation rates at 20.6 MHz of Mn(II)–CF_1 solutions containing 0, 10, 20, and 30 μM $MnCl_2$. Shown are the observed relaxation rates of the four solutions used for the field dependence study (open diamonds), the relaxation rates of solutions containing only the unbound Mn(II) at concentrations corresponding to those in the Mn(II)–CF_1 solutions [0, 0.7, 2.2, and 3.9 μM hexaaquo-Mn(II)] (closed diamonds), the relaxation rates of the Mn(II)–CF_1 solutions corrected for the contributions from free Mn^{2+} (closed squares), and the relaxation rates due to only the Mn(II)–CF_1 complex, corrected for both diamagnetic contributions and paramagnetic contributions from free Mn^{2+} (open squares).

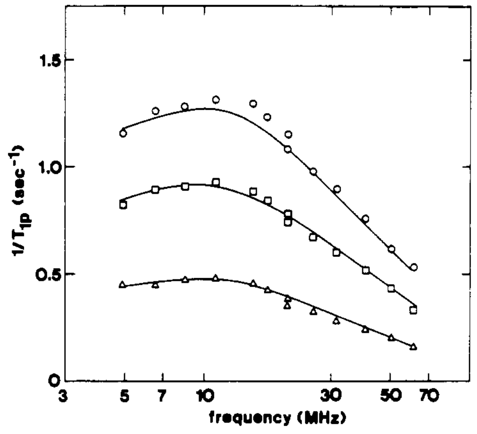

FIGURE 3: Magnetic field dependence of the paramagnetic spin–lattice relaxation rate ($1/T_{1p}$) of water protons for Mn(II) binding to CF_1. Measurements were made at 25 °C on solutions of 20 μM latent CF_1 with 10, 20, or 30 μM $MnCl_2$. The amounts of bound Mn(II) and corrections for relaxation contributions from water molecules not in contact with bound Mn(II) were calculated as described under Materials and Methods. The least-squres fits are represented by the solid curves. The ratios of Mn(II) bound per CF_1 were 0.47 (triangles), 0.89 (squares), and 1.3 (circles).

Proton NMR Relaxation Due to Mn(II)–CF_1. Proton NMR relaxation data were measured by using samples containing 20 μM latent CF_1 plus 0.50, 1.00, or 1.50 molar equiv of $MnCl_2$. Control samples, comprising the protein in buffer without added metal ion and Mn(II) plus buffer without CF_1, were run concurrently. Typical data obtained at 20.6 MHz are shown in Figure 2.

Table II: Nonlinear Least-Squares Fit Parameters for Mn(II) Bound to CF$_1$[a]

Mn$_b$/CF$_1$	τ_d (ps)	$1/\tau_{s,v} + 1/\tau_r$ (s^{-1})	$\tau_{s,d}^o$ (ns)	τ_m (ns)	q
0	100			326	1.09
0.47		0.95×10^8	1.82 (±120%)	342 (±7.9%)	1.13 (±3.9%)
0.89		1.05	1.23 (±65%)	343 (±6.5%)	1.17 (±3.5%)
1.3		1.15	1.23 (±85%)	364 (±8.8%)	1.20 (±5.0%)
1.3	50	1.15	4.30 (±97%)	365 (±9.1%)	1.20 (±5.2%)

[a] Data sets for which these parameters were calculated correspond to those shown in Figure 4. Values were assigned to $1/\tau_{s,v} + 1/\tau_r$ according to the average of the experimental deuteron $1/T_{1p}{}^d$ to proton $1/T_{1p}{}^p$ ratios for the samples of Table III. By setting the value of τ_d at 100 ps, the values of the other three parameters were generated by the nonlinear least-squares fitting procedure as described under Materials and Methods assuming r = 2.77 Å. A representative solution using τ_d = 50 ps is also shown for 1.3 Mn$_b$/CF$_1$. Errors represent standard deviations generated by the least-squares fitting procedure; for τ_{sd}^o, the tabulated value underestimates the true error (see text). The first row of the table represents extrapolations of q and τ_m to zero Mn$_b$/CF$_1$.

Table III: Comparison of Experimental and Calculated $1/T_{1p}$ Values for Deuterons and Protons for Mn(II) Bound to CF$_1$[a]

		$1/T_{1p}$, calcd		
Mn$_b$/CF$_1$	nucleus	fit 1	fit 2	$1/T_{1p}$, exptl
0.89	^{1}H	0.757	0.757	0.757 ± 0.007
	^{2}H	0.079	0.018	0.071 ± 0.023
1.3	^{1}H	1.161	1.161	1.161 ± 0.015
	^{2}H	0.123	0.028	0.135 ± 0.041

[a] Measurements of deuteron and proton relaxation rates were made at 25 °C on 200-μL solutions containing 20 μM latent CF$_1$, either 20 or 30 μM MnCl$_2$, and about 3/1 D$_2$O/H$_2$O solvent. The Larmor frequency of protons and deuterons was set to 12.63 MHz. Experimental deuteron relaxation rates represent averages of 75–80 measurements; experimental proton relaxation rates represent averages of 10 measurements. Errors were propagated from the standard deviations for the R_1 measurements in the absence and presence of added Mn(II). Fits 1 and 2 represent the two major minima of the proton dispersion profile least-squares analyses. Fit 1 corresponds to that given in Table II for either 0.89 or 1.3 Mn$_b$/CF$_1$. Fit 2 corresponds to the following: for 0.89 Mn$_b$/CF$_1$, τ_d = 100 ps, $\tau_{s,d}^o$ = 3.06 ns, τ_m = 3.58 ns, q = 0.447, and $1/\tau_{s,v} + 1/\tau_r = 0.3 \times 10^7$ s^{-1}; for 1.3 Mn$_b$/CF$_1$, τ_d = 100 ps, $\tau_{s,d}^o$ = 3.06 ns, τ_m = 3.31 ns, q = 0.462, and $1/\tau_{s,v} + 1/\tau_v = 0.3 \times 10^7$ s^{-1}. For the calculations, the Mn(II)–enzyme concentration, E, was adjusted to that of the experiments in Table II by comparing proton relaxation rates at 12.63 MHz.

Figure 3 shows magnetic field dispersion profiles of the ^{1}H R_1, measured between 4 and 62 MHz, for three Mn(II)/CF$_1$ binding ratios. The profiles show a mild local maxima near 12 MHz, resulting from field dependence in τ_{s1} for Mn(II). Results of the nonlinear least-squares analyses of the data are shown in Table II. The hydration numbers and the residence times were determined to better than ±10% in all cases. The motional correlation times, τ_d and $\tau_{s,d}^o$, are strongly covariant, and their absolute values are much more uncertain (compare the last two entries of Table II).

Comparative ^{1}H and ^{2}H data obtained at the same magnetic field strength using a single Mn(II)–CF$_1$ solution provided initial estimates of the manganese hydration number and solvent exchange lifetime via eq 8–10. These initial values were refined by least-squares analysis using the full ^{1}H data set. Final values for q and τ_m were within 30% of the starting values. These final parameters were then used to recalculate the ^{2}H R_1's, as shown by Table III (fit 1), to obviate possible confusion due to the existence of multiple error minima in the fitting procedure.

A second fit with acceptably low error does in fact exist for the data in Figure 3. In this fit, the hydration number is fractional, q = 0.6, and the residence lifetime is very short, τ_m = 5 ns. Both of these values seem nonphysical; a fractional hydration number is clearly difficult to explain, while the fitted solvent exchange lifetime is about an order of magnitude shorter than that of hexaaquo-Mn(II) and seems unreasonably small. The ^{2}H data provide a clear discrimination between the two fits (Table III). While the ^{1}H data are fit almost equally well by both parameter sets, the ^{2}H data are consistent only with the first set (that of Table II), thus confirming physical arguments given above supporting this choice.

DISCUSSION

Manganese Binding Sites on Nucleotide-Depleted CF$_1$. A single very high-affinity ADP binding site, termed site 1 by Leckband and Hammes (1987), has been found to resist depletion during the isolation and desalting procedures for CF$_1$. Quantitation of endogenous ADP (Table I) indicates that this site is occupied in our preparations. The amount of adenine nucleotide found upon initial isolation of the enzyme (1.1–1.3 mol of ADP and 0.1–0.2 mol of ATP per mole of CF$_1$) was similar to that found by other workers (Carlier & Hammes, 1979; Hiller & Carmeli, 1985). Substantial levels of endogenous Mg(II), approximately 1.3 mol/mol of CF$_1$, were also present in our preparations. The level of Mg(II) is equimolar with total endogenous nucleotide (ADP + ATP) within the measurement error, suggesting that tightly bound ADP may be present as a Mg(II)–ADP complex. Approximately equimolar levels of endogenous AdN and Mg have been found by Hiller and Carmeli (1985) and by Girault and coworkers (Girault et al., 1982).

Site 2 of Leckband and Hammes (1987) binds Mg(II)–ATP with very high affinity, in a manner that withstands prolonged gel filtration. This site is normally largely depleted in enzyme which has been precipitated with (NH$_4$)$_2$SO$_4$ (Bruist & Hammes, 1981), such as during storage. In our CF$_1$ preparations, this site appears to be partially occupied. Endogenous AdN was present in significant molar excess over CF$_1$ [approximately 1.3 mol of (ADP + ATP)/mol of CF$_1$], with Mg(II)–ATP accountable for much of the excess. In accord with these results, we interpret the endogenous Mg(II) and AdN levels in our enzyme as indicative of 1.0 molar equiv of Mg(II)–ADP in site 1 and 0.2 molar equiv of Mg(II)–ATP in site 2. Residual traces of Mg(II)–ADP may also occupy site 2 and/or 3.

Addition of MnCl$_2$ to nucleotide-depleted CF$_1$ results in the high-affinity binding of 0.7 mol of Mn(II)/mol of CF$_1$, bringing the total bound divalent metal ion to 2.0 mol/mol of CF$_1$. The presence of very tightly bound Mn(II) is likewise evident in the ESR data of Figure 1, where approximately 0.5 molar equiv of Mn(II) bound to CF$_1$ and equilibrated with less than 1 μM Mn^{2+} in the aqueous phase. This population of tightly bound Mn(II) evidently corresponds to the nonlabile Mn(II) binding site that resists depletion by gel filtration over Sephadex G-50. The total measured Mn(II) + Mg(II) indicates the presence of two nonlabile divalent metal binding sites on nucleotide-depleted CF$_1$.

In addition to the nonlabile binding sites, at least one additional labile high-affinity Mn(II) site is present, with a dissociation constant in the low micromolar range (Figure 1).

This brings the total number of high-affinity divalent cation [Mn(II) + Mg(II)] binding sites to at least 3. While some of these sites may be occupied by metal–nucleotide complexes, the experimental metal–AdN to CF_1 stoichiometry is no more than 1.4 mol/mol; thus, at least one and probably two types of high-affinity binding sites exist for divalent metal ions unaccompanied by nucleotide. It is these manganese binding sites which do not contain nucleotide that are the subject of the present study.

Properties of the High-Affinity Mn(II) Binding Sites. Properties of the Mn(II) binding sites have been inferred from an analysis of the magnetic field dependent ^1H and ^2H NMR data, and the results are summarized in Table II. The fitting parameters were determined as a function of added Mn(II) and extrapolated to zero binding ratio of Mn(II) to CF_1 (Table II). The tightest binding site for added Mn^{2+} (that at zero added $MnCl_2$) is exposed to the solvent and contains a single exchangeable water molecule in its coordination sphere. The mean lifetime prior to chemical exchange, τ_m, is approximately 330 ns. This value is 5–10 times longer than that for $Mn(H_2O)_6^{2+}$ (Bernheim et al., 1959) but is comparable to values reported for other mangano-enzymes (Koenig et al., 1971; Brown et al., 1977).

The spin–lattice relaxation time of the electron spin was also determined in these experiments and provides a measure of chemical asymmetry at the Mn(II) binding site (see below). The value at low field is $\tau_{s1}^{\circ} = 1/[(\tau_{s,v})^{-1} + (\tau_{s,d}^{\circ})^{-1}] = 1$ ns at 25 °C (this value is rough owing to a factor of 2 uncertainty in $\tau_{s,d}^{\circ}$). τ_{s1}° is fairly long, a factor of only 3–4 shorter than that for $Mn(H_2O)_6^{2+}$ (Bloembergen & Morgan, 1961), and it is an order of magnitude longer than τ_{s1}° for the tight Mn(II) site in ternary Mn(II)–ADP–CF_1 and Mn(II)–ATP–CF_1 complexes (Haddy et al., 1989). The long τ_{s1}° corresponds to high site symmetry (i.e., small static zero field splittings) for the bound metal ion in the binary Mn(II)–CF_1 complex.

Statistical errors were ±5% for the hydration number, q, and ±9% for the mean residence time, τ_m, based on a multiparameter fit to the four parameters. It should be noted that q is very sensitive to the value assumed for the distance r. However, a large displacement of the electron spin from the metal center, of more than 0.3 Å, would be required to account for an integral value of q other than 1. We can also rule out the possibility that q was influenced by Mn(II) binding to low-affinity sites. At the Mn^{2+} concentrations used, very little binding occurred at the low-affinity sites, and previous work (Haddy et al., 1985) has shown that the relaxation enhancement is similar to that for the high-affinity sites; thus, the relaxation rates observed reflect binding of Mn(II) to the high-affinity sites.

Further information on the tightest Mn(II) binding site is available from a recent manganese EXAFS study of latent Mn(II)–CF_1 (Carmeli et al., 1986). These authors reported 4.2 ± 1 nearest-neighbor CNO atoms at 2.05 Å with no outer sphere diffraction from phosphorus out to 5 Å. These results, in conjunction with the measured hydration number and with the high symmetry that is implied by the long measured value of τ_{s1}° (see above), are consistent with approximate tetrahedral site symmetry with three protein ligands plus a single exchangeable water.

The concentration dependence of the parameters are quite small (Table II). Labile (readily exchangeable) Mn(II) which bound beyond the nonlabile 0.7 Mn(II) per CF_1 (Table I and Figure 1) apparently occupied a site that was NMR visible in the relaxation data and had enhancement parameters similar to those of the nonlabile Mn(II) (Table II). Thus, the second labile Mn(II) site likewise had a single exchangeable water, and its correlation times (τ_m, $\tau_{s,v}$, and $\tau_{s,d}^{\circ}$) were quite similar to those of the first site. This similarity in properties is striking: the proton relaxation data depend strongly on τ_{s1} and are therefore quite sensitive to perturbations of symmetry in the crystal field of the metal ion. A previous study by NMR proton relaxation enhancement (Haddy et al., 1985) had likewise shown the existence of two to three interacting classes of high-affinity Mn(II) binding sites, for which the relaxation enhancement parameters are very similar.

A possible explanation of the observed similarity of the sites is that added Mn(II) binds to unoccupied nucleotide binding sites. Two binding sites, corresponding to sites 2 and 3 of Leckband and Hammes (1987) in nucleotide binding experiments, are largely unoccupied in our CF_1 preparations. These sites may, in the absence of nucleotide, bind 2 molar equiv of added Mn(II) in environments that are chemically similar. It is well-known that the tight nucleotide sites differ in their binding affinities toward nucleotides and that they are strongly coupled (Hackney et al., 1979). However, at least two and probably all three nucleotide sites appear to lie on β subunits (Admon & Hammes, 1987; Abbott et al., 1984; Bar-Zvi & Shavit, 1984; Czarnecki et al., 1985), in regions of similar primary sequence (Admon & Hammes, 1987), and they may exhibit very similar properties when occupied by Mn(II). The number of high-affinity manganese sites correlates with the number of empty nucleotide sites, and positive cooperativity between the Mn(II) binding sites has been observed (Haddy et al., 1985; Hiller & Carmeli, 1985).

Related observations which appear to be consistent with the notion that Mn(II) may bind at empty nucleotide binding sites involve the well-known inhibition of ATPase activity by excess Mg(II) or Mn(II) and the relief of Mg(II)-dependent inhibition by EDTA treatment. Mn(II) is a competitive inhibitor of ATPase activity with a K_i in the range 1–10 μM (Hochman et al., 1976; Hochman & Carmeli, 1981a). Removal of tightly bound Mg(II) correlates kinetically both with the reactivation of ATPase activity and with the binding of added ADP (Feldman & Boyer, 1985). This result is consistent with the notion that metal ion bound to an empty nucleotide binding site prevents the oocupation of that site by nucleotide, thereby inhibiting catalysis.

A further test of this hypothesis can be based on an examination of the R_1 dispersion profiles of ternary Mn(II)–AdN–CF_1 complexes, specifically to address the question of whether Mn(II) bound in the sites described above is displaced by added nucleotide, or is at least profoundly influenced with respect to its chemical environment. This is the subject of the following paper (Haddy et al., 1989).

Accuracy of SBM Theory. It is of interest to consider the range of validity of the SBM theory when applied to Mn(II)–CF_1 as described above. The original formulation of the theory was intended to model proton relaxation in solutions of $Mn(H_2O)_6^{2+}$, where Mn(II) lies in a site of approximately cubic static site symmetry. Mn(II) is an $S = {}^5/_2$ ion for which zero-field splittings tend to be quite small. The spin relaxation of protons that are coordinated to the metal ion depends on the spectral density of the dipolar interaction at the ^1H transition frequencies in the coupled spin system:

$$\frac{1}{T_{1m}} = \frac{B}{r^6}[3j(\omega_I) + 6j(\omega_I + \omega_s) + j(\omega_I - \omega_s)] \quad (11)$$

In SBM theory, the electronic interaction is assumed to be dominated by the Zeeman interaction, i.e., $H_Z \gg H_{ZFS}$. When the magnetic field strength is low and the metal binding site asymmetric, this condition may no longer hold, the corrections for the nonzero ZFS may be required (Koenig et al., 1973). The first term in eq 11, $j(\omega_I)$, describes the longitudinal component of coupling between the I and S spins (Koenig, 1978) and retains the SBM form irrespective of the magnitude of zero-field splittings. The terms in $\omega_{I\pm S}$ describe two quantum transitions of the coupled spin system. It is these latter terms that require correction.

Over the range of magnetic field strengths employed here ($H_0 > 0.1$ T), the electronic Larmor frequency is large enough that $\omega_s\tau_s \gg 1$, and relaxation contributions at the electronic transitions have largely dispersed away, and thus the electronic transition frequencies exert no observable effect on $1/T_{1m}$. Direct experimental confirmation that $\omega_s \gg \tau_{s1}$ is evident in the functional form of the dispersion profile of Figure 3. The fact that R_1 passes through a local maximum, as opposed to declining monotonically with increasing field strength, clearly implies that the dipolar correlation time is strongly field dependent, i.e., that it must be identified with τ_{s1} in its field-dependent region and that the observed R_1 dispersion is dominated by $j(\omega_I)$. This provides confirmation of the applicability of eq 3 and 8 in the magnetic field range employed.

A modification to the standard SBM theory, specifically, the use of two motional correlation times to describe fluctuations in the ligand field (eq 5), was used and greatly improved the ability of theory to fit the combined ^{1}H and ^{2}H data. A more complex form of the spectral density function than that suggested by Bloembergen and Morgan (1961) is physically reasonable for metalloenzymes. Effects of the low-frequency terms ($\tau_d > 50$ ps) are clearly important since they are responsible for the observed field dependence of $\tau_{s1}{}^{\circ}$ and the corresponding local maximum in the dispersion profile. The constant high-frequency term, $1/\tau_{s,v}$, was not required for a satisfactory fit of only the ^{1}H data (although such a fit is physically incorrect as shown in Table III), but it was required for simultaneous fit to both ^{1}H and ^{2}H data. This term appears in the sum $1/\tau_m + 1/\tau_r + 1/\tau_{s,v}$ and can be masked unless τ_m is strongly defined. When ^{2}H data are available and τ_m is within an order of magnitude of T_{1m}, τ_m is determined independently through eq 9, and inclusion of $\tau_{s,v}$ (or an analogous field-independent correlation time) is essential to a satisfactory fit of the data. Of course, a highly accurate description may not be possible with only two correlation times, but it appears that an expression minimally of the form of eq 5 is necessary to achieve a satisfactory fit to both ^{1}H and ^{2}H R_1 data.

The results in Table III clearly illustrate the deficiency of the traditional SBM approach in which a single correlation time is used to describe fluctuations of the ligand field. "Fit 2" in the table, which assumed $\tau_{sv}{}^{-1} = 0$, gave an unphysically short τ_m, a fractional hydration number, and predicted ^{2}H relaxation rates much smaller than those observed.

ACKNOWLEDGMENTS

We thank Wayne D. Frasch for helpful discussions.

Registry No. ATPase, 9000-83-3; Mn, 7439-96-5; ATP synthase, 37205-63-3.

REFERENCES

Abbott, M. S., Czarnecki, J. J., & Selman, B. R. (1984) *J. Biol. Chem. 259*, 12271–12278.

Admon, A., & Hammes, G. G. (1987) *Biochemistry 26*, 3193–3197.

Banai, M., Shavit, N., & Chipman, D. M. (1978) *Biochim. Biophys. Acta 504*, 100–107.

Bar-Zvi, D., & Shavit, N. (1984) *Biochim. Biophys. Acta 765*, 340–346.

Bernheim, R. A., Brown, T. H., Gutowsky, H. S., & Woessner, D. E. (1959) *J. Chem. Phys. 30*, 950–956.

Bertini, I., Luchinat, C., Mancini, M., & Spina, G. (1984) *J. Magn. Reson. 59*, 213–222.

Bloembergen, N., & Morgan, L. O. (1961) *J. Chem. Phys. 34*, 842–850.

Brown, R. D., Brewer, C. F., & Koenig, S. H. (1977) *Biochemistry 16*, 3883–3896.

Bruist, M. F., & Hammes, G. G. (1981) *Biochemistry 20*, 6298–6305.

Cantley, L. C., & Hammes, G. G. (1975) *Biochemistry 14*, 2968–2975.

Carlier, M.-F., & Hammes, G. G. (1979) *Biochemistry 18*, 3446–3451.

Carmeli, C., Huang, J. Y., Mills, D. M., Jagendorf, A. T., & Lewis, A. (1986) *J. Biol. Chem. 261*, 16969–16975.

Czarnecki, J. J., Dunham, K. R., & Selman, B. R. (1985) *Biochim. Biophys. Acta 809*, 51–56.

Dwek, R. A. (1973) in *Nuclear Magnetic Resonance (NMR) in Biochemistry*, pp 202–210, Clarendon Press, Oxford.

Feldman, R. I., & Boyer, P. D. (1985) *J. Biol. Chem. 260*, 13088–13094.

Frasch, W. D., & Selman, B. R. (1982) *Biochemistry 21*, 3636–3643.

Girault, G., Galmiche, J.-M., Michel-Villaz, M., & Thiery, J. (1973) *Eur. J. Biochem. 38*, 473–478.

Girault, G., Galmiche, J.-M., LeMaire, C., & Stulzaft, O. (1982) *Eur. J. Biochem. 128*, 405–411.

Hackney, D. D., Rosen, G., & Boyer, P. D. (1979) *Proc. Natl. Acad. Sci. U.S.A. 76*, 3646–3650.

Haddy, A. E., Frasch, W. D., & Sharp, R. R. (1985) *Biochemistry 24*, 7926–7930.

Haddy, A. E., Frasch, W. D., & Sharp, R. R. (1989) *Biochemistry* (following paper in this issue).

Hiller, R., & Carmeli, C. (1985) *J. Biol. Chem. 260*, 1614–1617.

Hochman, Y., & Carmeli, C. (1981a) *Biochemistry 20*, 6287–6292.

Hochman, Y., & Carmeli, C. (1981b) *Biochemistry 20*, 6293–6297.

Hochman, Y., Lanir, A., & Carmeli, C. (1976) *FEBS Lett. 61*, 255–259.

Karplus, M., Swaminathan, S., Ichiye, T., & Van Gunsteren, W. F. (1983) *Ciba Found. Symp. 93*, 271–290.

Koenig, S. (1978) *J. Magn. Reson. 31*, 1–10.

Koenig, S. H., Brown, R. D., & Studebaker, J. (1971) *Cold Spring Harbor Symp. Quant. Biol. 36*, 551–559.

Koenig, S. H., Brown, R. D., & Brewer, C. F. (1973) *Proc. Natl. Acad. Sci. U.S.A. 70*, 475–479.

Lanir, A., Gradstajn, S., & Navon, G. (1975) *Biochemistry 14*, 242–248.

Leckband, D., & Hammes, G. G. (1987) *Biochemistry 26*, 2306–2312.

Levanon, H., Charbinsky, S., & Luz, Z. (1970a) *J. Chem. Phys. 53*, 3056–3064.

Levanon, H., Stein, G., & Luz, Z. (1970b) *J. Chem. Phys. 53*, 876–887.

Lowry, O. H., Rosenbrough, N. J., Farr, A. L., & Randall, R. J. (1951) *J. Biol. Chem. 193*, 265–275.

McGarvey, B. R. (1957) *J. Phys. Chem. 61*, 1232–1237.

Moroney, J. V., Lopresti, L., McEwen, B. F., McCarty, R. E., & Hammes, G. G. (1983) *FEBS Lett. 158*, 58–62.

Navon, G. (1970) *Chem. Phys. Lett. 7*, 390–394.

Schinkel, J. E., & Hammes, G. G. (1986) *Biochemistry 25*, 4066–4071.
Sharp, R. R. (1972) *J. Chem. Phys. 57*, 5321–5330.
Williamson, J. R., & Corkey, B. E. (1969) *Methods Enzymol. 8*, 434–513.
Yocum, C. F., Yerkes, C. T., Blankenship, R. E., Sharp, R. R., & Babcock, G. T. (1981) *Proc. Natl. Acad. Sci. U.S.A. 78*, 7507–7511.

Properties of the Manganese(II) Binding Site in Ternary Complexes of Mn•ADP and Mn•ATP with Chloroplast Coupling Factor 1: Magnetic Field Dependence of Solvent ^{1}H and ^{2}H NMR Relaxation Rates[†]

Alice E. Haddy,[‡] Wayne D. Frasch,[*,§] and Robert R. Sharp[*,‡]
Department of Chemistry and Division of Biological Sciences, The University of Michigan, Ann Arbor, Michigan 48109

Received July 19, 1988; Revised Manuscript Received November 18, 1988

ABSTRACT: The influence of the binding of ADP and ATP on the high-affinity Mn(II) binding site of chloroplast coupling factor 1 (CF_1) was studied by analysis of field-dependent solvent proton and deuteron spin–lattice relaxation data. In order to characterize metal–nucleotide complexes of CF_1 under conditions similar to those of the NMR experiments, the enzyme was analyzed for bound nucleotides and Mn(II) after incubation with AdN and $MnCl_2$ and removal of labile ligands by extensive gel filtration chromatography. As isolated, the enzyme contained 1.3–1.4 mol of adenine nucleotide (mostly ADP) and 1.3 mol of Mg(II) per mole of CF_1. After incubation with added Mn(II) and nucleotide, a total of three binding sites with high affinity for divalent metal ions (Mg^{2+} + Mn^{2+}) and/or nucleotide (ATP or ADP) were found. In the field-dependent NMR experiments, the Mn(II) binding site of CF_1 was studied for three mole ratios of added Mn(II) to CF_1, 0.5, 1.0, and 1.5, in the presence of an excess of either ADP or ATP. The results were extrapolated to zero Mn(II) concentration to characterize the environment of the first Mn(II) binding site of CF_1. In the presence of both adenine nucleotides, pronounced changes in the Mn(II) environment relative to that in Mn(II)–CF_1 were evident; the local relaxation rate maxima were more pronounced and shifted to higher field strengths, and the relaxation rate per bound Mn(II) increased at all field strengths. Analysis of the data revealed that the number of exchangeable water molecules liganded to bound Mn(II) increased from one in the binary Mn(II)–CF_1 complex to three and two in the ternary Mn(II)–ADP–CF_1 and Mn(II)–ATP–CF_1 complexes, respectively; these results suggest that a water ligand to bound Mn(II) in the Mn(II)–ADP–CF_1 complex is replaced by the γ-phosphate of ATP in the Mn(II)–ATP–CF_1 complex. The residence time of water within the inner coordination sphere was found to be 430 ns in the presence of ADP and 260 ns in the presence of ATP. The low-field electron spin relaxation time decreased in the ternary Mn(II)–AdN–CF_1 complexes relative to binary Mn(II)–CF_1, reflecting a lower Mn(II) site symmetry in the latter complex. A binding model is presented to account for these observations.

The requirement for a divalent metal in the synthesis and hydrolysis of ATP by chloroplast coupling factor 1 (CF_1)[1] suggests that the presence of adenine nucleotides should have a marked effect on the environment of enzyme-bound metal. The metal cofactor participates as a metal–nucleotide complex in the ATPase reaction of CF_1 (Hochman & Carmeli, 1981; Leckband & Hammes, 1987). Studies with exchange-inert Cr(III)–nucleotides have shown that the substrate for ATP hydrolysis is a tridentate metal–ATP complex while the substrate for ATP synthesis is the Λ-bidentate metal–ADP complex (Frasch & Selman, 1982); these results suggest that the metal ion remains coordinated to the phosphate oxygens throughout the hydrolysis reaction.

We have previously analyzed the magnetic field dependence of NMR relaxation rates of solvent protons and deuterons as a probe of the coordination environment of CF_1-bound Mn(II) (Haddy & Sharp, 1989). The present study extends this investigation from the binary Mn(II)–CF_1 complex to ternary complexes of Mn(II)–ADP–CF_1 and Mn(II)–ATP–CF_1. In each case, attention has been focused on the high-affinity Mn(II)-containing complexes in the given binary or ternary system. For this purpose, relaxation data have been collected as a function of added Mn(II) in the presence of excess nucleotide and the results of the analysis extrapolated to zero Mn(II)/CF_1 binding ratio. Measurements of the magnetic field dependence (the field dispersion profile) of the NMR spin–lattice relaxation rate, R_1, of solvent protons permit a determination of the metal ion hydration number and of the residence time of solvent molecules which exchange between the bulk aqueous phase and ligand sites in the Mn(II) coordination sphere. The analysis also characterizes magnetic interactions within the Mn(II) coordination sphere, specifically the spectral density function describing the dipolar interaction between electron and proton spins.

[†] This work was supported by the U.S. Department of Agriculture in the form of a research grant (CRCR 1 1339) to R.R.S. and W.D.F. and by the Herman Frasch Foundation of the American Chemical Society (0188 HF) to W.D.F.

[*] Author to whom correspondence should be addressed.

[‡] Department of Chemistry.

[§] Division of Biological Sciences.

[1] Abbreviations: CF_1, chloroplast coupling factor 1; AdN, adenine nucleotide.